

Order-Chaos Transition of Two Trapped Ions

J. Hoffnagle,⁽¹⁾ R. G. DeVoe,⁽¹⁾ L. Reyna,⁽²⁾ and R. G. Brewer⁽¹⁾

⁽¹⁾IBM Research Division, Almaden Research Center, San Jose, California 95120-6099

⁽²⁾IBM Research Division, T. J. Watson Research Center, Yorktown Heights, New York 10598

(Received 8 April 1988)

Phase transitions of trapped particles and ions, observed initially in 1959 by collisional cooling and recently by laser cooling, are explained as order-chaos transitions. Here, two trapped Ba⁺ ions are examined experimentally and by computer solution of the equations of motion. The ordered state, quasi-periodic with two frequencies, becomes chaotic when a bifurcation introduces a third frequency at a critical value of a control parameter. This route evolves from the nonlinear Coulomb coupling of the ion pair's axial and radial motions, displaying frequency locking and hysteresis, which is observed.

PACS numbers: 05.45.+b, 05.70.Fh, 32.80.Pj, 42.50.Vk

In 1959¹ Wuerker, Shelton, and Langmuir observed a phase transition of charged aluminum particles stored in a Paul or radio-frequency electric quadrupole trap. The particles assumed an ordered array, a crystalline state, when cooled by collisions with a background gas, but a disordered state, characterized by a random motion with large orbits, occurred when a control parameter achieved a critical value. Recently, small numbers of laser-cooled trapped ions have been observed to exhibit an ordered state^{2,3} and a transition² to a disordered state with hysteresis.

In this Letter, we present theoretical and experimental evidence for this phenomenon being an order-chaos transition, an interpretation not considered previously. In our view, the ion-trap system is deterministic, rather than stochastic, since the relevant equations of motion

contain a radio-frequency driving term, dissipation, and a Coulomb term which couples the ions nonlinearly—ingredients that should lead to chaos.^{4,5} We show that the particles can execute a complicated motion in the sense of a *strange attractor* while still remaining bound to the trap. It is often remarked that the transition to chaos is *analogous* to a phase transition, for example, to a spin-ordering ferromagnetic transition, but in the present instance an analogy is not required because the two phenomena coincide.

We have approached this problem by treating the simplest case, that of two trapped ions having the same charge e and mass m , this being one of the few examples of chaos in a two-particle system. We write the scaled classical equations of motion for the *relative* motion of an ion pair as

$$\begin{aligned} d^2z/dx^2 + \Gamma dz/dx + z[-\alpha/(r^2+z^2)^{3/2} + 2q \cos 2x] + \text{noise} &= 0, \\ d^2r/dx^2 + \Gamma dr/dx - r[\alpha/(r^2+z^2)^{3/2} + q \cos 2x] + \text{noise} &= 0, \end{aligned} \quad (1)$$

where (z, r) refers to the trap's axial and radial coordinates and the trap potential $V = V_{ac}(\cos \Omega t)(z^2 - r^2/2)/\bar{r}_0^2$, V_{ac} being the applied peak rf voltage and \bar{r}_0 the trap radius.¹ The scaled time variable is $x = \Omega t/2$, where Ω is the micromotion angular frequency, and hence $\cos 2x$ signifies a driving term where the control parameter $q \equiv 4eV_{ac}/(m\Omega^2\bar{r}_0^2)$. For the Coulomb term, $\alpha \equiv e^1/(m\Omega^2)$. The problem is two-dimensional because we assume that the angular momentum about the z axis is zero. On the other hand, the center-of-mass motion is described by two Mathieu equations which do not contain the Coulomb term and, therefore, cannot lead to chaos. The significance of the noise terms is discussed below.

The damping terms in (1) are appropriate for collisional cooling as the Wuerker, Shelton, and Langmuir experiments and are suitable as a first approximation to laser cooling. However, new features emerge, which makes the problem more complex, when these terms are replaced by the scaled damping force due to laser cool-

ing,⁶

$$\mathbf{F}_{z,r} = 4\hbar \mathbf{k}_{z,r} \gamma \rho_{22}(\Delta, \chi, R)/(m\Omega^2). \quad (2)$$

Equation (2) expresses the rate of change of the recoil momentum $\hbar k$ of the ion pair due to repeated resonant optical absorption-emission cycles—a short-time average over several cycles where γ is the spontaneous emission decay rate. Here, $\mathbf{k}_{z,r}$ is the optical propagation vector projected along the z or r directions. Quantum-mechanical solutions of the idealized two-state ion yield ρ_{22} , the ion's excited-state diagonal density matrix element which is not only a function of the tuning parameter Δ and the Rabi frequency χ , scaled by the factor $2/\Omega$, but also the ion pair's time-dependent position vector $\mathbf{R} = \mathbf{r} + \mathbf{z}$. In this way, the two-state semiclassical equations of motion are coupled to Eq. (1). Since $1/\gamma$ is usually the fastest time scale encountered, the steady-state solution

$$\rho_{22} = (\chi^2/4)/\{[\Delta - \mathbf{k} \cdot (\mathbf{r} + \mathbf{z})]^2 + (\gamma/2)^2 + (\chi^2)/2\},$$

which is velocity dependent, agrees closely with exact numerical results.⁷

In the small- q regime, a perturbation calculation of (1) can be performed by separating the fast micromotions and the slow secular motions and by expanding the Coulomb terms about the equilibrium position $z_0=0$ and $r_0=2(a/q^2)^{1/3}$. Interestingly, the Coulomb interaction makes the radial and axial secular frequencies equal, $\omega_z = \omega_r = q\sqrt{3/8}$ or in ordinary units $(q\Omega/2)\sqrt{3/8}$. In contrast, the center-of-mass solutions of the Mathieu equations result in $\omega_z = 2\omega_r = q/\sqrt{2}$.

Computer solutions of (1), or in combination with (2), show that as q approaches the transition point q_c from the ordered state, transients decay smoothly to their equilibrium value where the Poincaré diagram \dot{r} vs r yields an attractor with a simple limit cycle, Fig. 1(a). Here, the ion pair displays quasiperiodicity with two frequencies, the micromotion (Ω) and secular frequencies ($\omega_z = \omega_r$). As q continues to increase, the Coulomb interaction couples the z and r motions more strongly, and a long-lived transient beat results prior to equilibrium, the energy alternating between the two motions. At the critical value q_c , the z, r coupling is strong enough to induce the transition to chaos. The explosive onset of chaos in Fig. 1(b) demonstrates not only an erratic temporal dependence with a dramatic increase in the z, r amplitudes but also that a radial bifurcation has occurred with a new equilibrium position centered on $r_0=0$, Fig. 1(c). (Negative r implies the ions exchange positions.) The computer snapshots of Fig. 2 catch the corresponding erratic spatial patterns that alternate in time. In addition, the first return maps of r and z show a

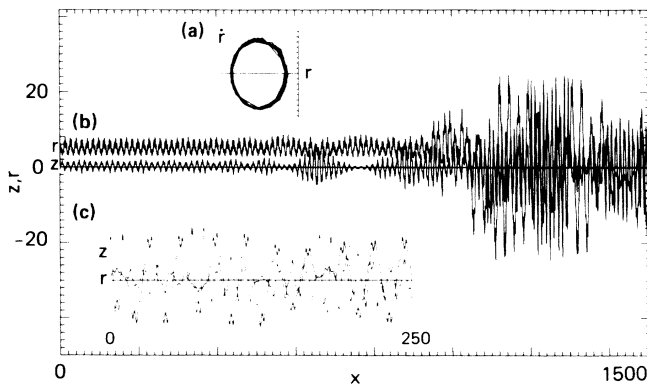


FIG. 1. Computer calculations for the case $q=0.73$ and $\alpha=16.2$ with laser damping parameters $\Delta = -20$, $\chi=30$, and $\nu=12.5$, and the peak r, z noise is $1.2 \mu\text{m}$. (a) The limit cycle \dot{r} vs r which characterizes the ordered state is centered on the equilibrium ion-ion distance $r_0=2(a/q^2)^{1/3}$. (b) The time development of r, z showing equal secular frequencies $\omega_z = \omega_r$ and transient beats prior to a chaotic explosion. (c) Chaotic behavior on an expanded time scale showing a bifurcation in r with oscillations about $r_0=0$ where $\Omega:\omega_z:\omega_r \cong 10:2:1$.

characteristic fuzziness and structure associated with chaos. We calculate that the Liapunov exponent, which is another measure of chaos, changes sign at q_c as expected with magnitude $\lambda = 30$.

At the equilibrium positions (r_0, z_0) , $z_0=0$ and the radial motion oscillates about r_0 at the micromotion frequency. As a result, the axial and radial motions do not interact, and thus, chaos cannot occur via this route. The role of noise in Eq. (1) is to displace the ions from equilibrium, changing the initial conditions but not the deterministic behavior that follows. In the Wuerker, Shelton, and Langmuir experiments, noise arises from neutral atom-particle collisions, but in laser cooling, fluctuations in ion recoil due to spontaneous emission appear and induce motions of about $0.2 \mu\text{m}$ which is sufficient to couple r and z in the route to chaos. Thus, noise triggers the initial r, z interaction which then develops dynamically in a deterministic way.

Some physical insight into the nature of the transition can be gained by the expansion of the Coulomb term about the equilibrium position $r_0=0$, $z_0=(2a/q^2)^{1/3}$. The leading radial terms correspond to a double potential well of the form $V = -\delta r^2 + \beta r^4$.⁸ The two ions can now exchange positions, hopping back and forth between the two wells, erratically at times and regularly at other times with a radial period $\sim \sqrt{3}$ times larger than the ordered state, Fig. 1(c), where $\omega_r \cong q/2\sqrt{2}$, the frequency of a single ion, since the ions are far apart much of the time in the chaotic state making the Coulomb terms in (1) small. This bifurcation breaks the degeneracy of the r, z motion that existed for $q < q_c$ [compare the attractors of Figs. 1(a) and 4(b)], and chaotic motion follows in the spirit of the Ruelle-Takens model.⁹

In addition, a rich variety of other phenomena are encountered such as hysteresis^{4,10} and frequency locking,¹¹ either for Eq. (1) alone or in combination with Eq. (2). On reducing q from the chaotic regime, the hysteresis

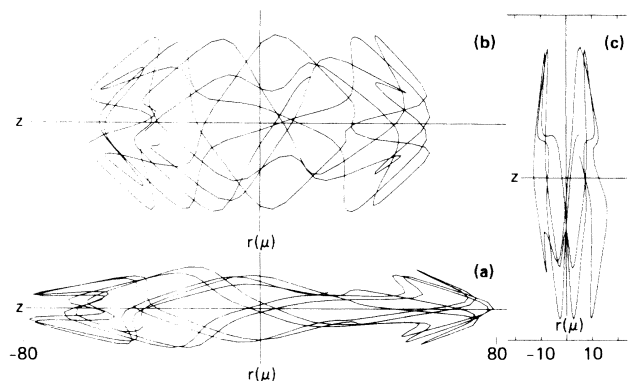


FIG. 2. Computer snapshots of chaotic z, r spatial patterns where the conditions are the same as Fig. 1 but the time window $x = 100$.

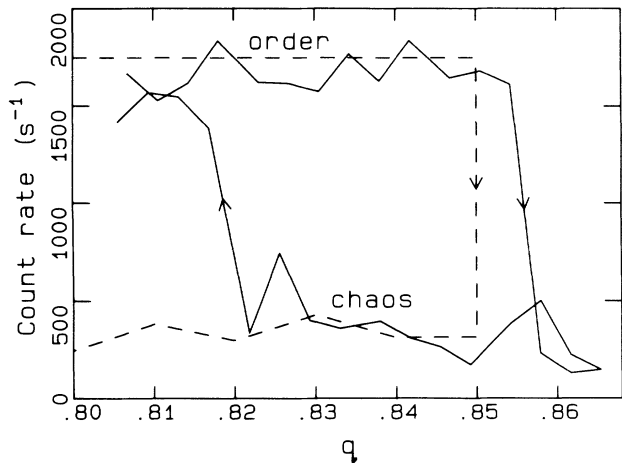


FIG. 3. Hysteresis loops of the photon count rate vs the control parameter q . Experimental: solid line; computer solutions of Eq. (1) where $\Gamma=2 \times 10^{-4}$ and the peak r, z noise is 0.2 microns: dashed line.

loop of Fig. 3 appears. Frequency locking occurs in windows of q , either in the return branch of these loops or when $q > q_c$. The simplest and first example to appear is the *dumbbell* attractor, Fig. 4(b), where the frequencies are locked in the integral ratios $\Omega:\omega_z:\omega_r=10:2:1$, revealed by its temporal behavior, Fig. 4(c). Its elongated spatial pattern, Fig. 4(a), is also distinctive with a double threaded path and two *bird's heads*, an interesting possibility for observation. At higher q 's, more complicated

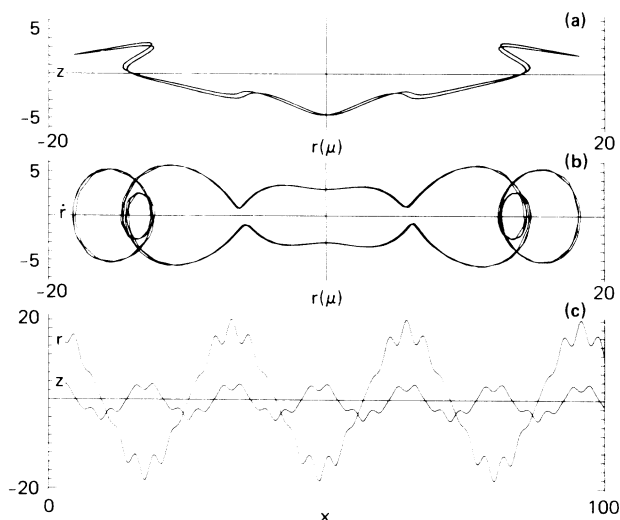


FIG. 4. Frequency locking of the *dumbbell* attractor, appearing on the return branch of a hysteresis loop. Computer solutions of Eq. (1) for (a) z vs r , (b) \dot{r} vs r , and (c) r, z vs x where the micromotion and secular frequencies are locked in the integral ratios $\Omega:\omega_z:\omega_r=10:2:1$ and $q=0.6$, $\alpha=16.2$, and $\Gamma=0.002$.

attractors appear, and between the windows, the motion seems to be random, that of a *strange attractor* where Figs. 2(a) and 2(b) appear to be aberrational versions of Fig. 4(a).

On the experimental side, the spatial behavior of two trapped and laser-cooled barium ions (Ba^+)¹² was examined below and above the transition points (q_c, q'_c) of the hysteresis loops. The electric quadrupole trap of radius $\bar{r}_0=0.25$ cm was driven at a frequency of 3.55 MHz. The background trap pressure was 10^{-9} Torr. The ion pair was detected by scattered laser light at 493.4 nm, the $6^2P_{1/2} \rightarrow 6^2S_{1/2}$ transition, and was also cooled when resonantly excited by a cw dye laser tuned to the red of line center at $\Delta = -20$ or -35 MHz, the natural linewidth being 11-MHz HWHM. Simultaneous excitation by a second collinear cw beam at 649.9 nm, the $5^2D_{3/2} \rightarrow 6^2P_{1/2}$ transition, avoided loss of ions to the $5^2D_{3/2}$ state. Both beams were focused to a $75\text{-}\mu\text{m}$ beam waist at the trap center and had powers of about $100\ \mu\text{W}$, the Rabi frequency of the blue beam being $\chi=64$ or 7.2×10^8 rad/s. The scattered light was viewed at an angle of 55° to the trap's z axis, and the ion pair's image was magnified 50 times before falling in a surface science imaging photon detector, with a count rate of $1000\ \text{s}^{-1}$ per ion and a background of $50\ \text{s}^{-1}$.

For $q < q_c$, the Ba^+ ion pair is in the ordered state, as in Fig. 5(a) where the calculated and observed ion-ion distances are $2z_0=2[2a/(q^2+4a)]^{1/3}=8.9$ and $10.5\ \mu\text{m}$, respectively. To improve the presentation, the ions are aligned³ parallel to the z axis by applying a 60-V dc field between the end caps and the ring where the parameter $a=qV_{dc}/V_{ac}$, although normally $V_{dc}=0$. By slowly increasing V_{ac} and hence q , the transition to chaos occurs at $q_c=0.85 \pm 0.01$, Fig. 3. On entering the chaotic region, the ion pair becomes an elongated cloud, about $40 \times 15\ \mu\text{m}^2$ and oriented radially usually as in Fig. 5(b) (compare Fig. 2). As q decreases on the return branch, a narrow hysteresis loop occurs with a transition to the

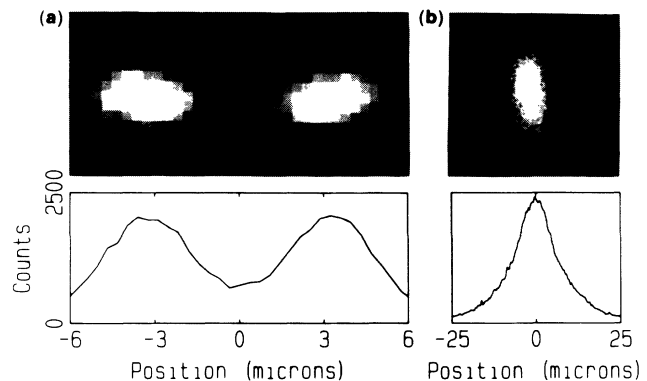


FIG. 5. Observed spatial patterns for two trapped Ba^+ ions in (a) the ordered state [$V_{ac}=401\ \text{V(rms)}$; $V_{dc}=59.6\ \text{V}$] and (b) the chaotic state [$V_{ac}=680\ \text{V(rms)}$; $V_{dc}=0$].

ordered state at $q'_c = 0.82 \pm 0.02$. Since the ions remain bound, the hysteresis can be reproduced as often as desired. Similarly, for three Ba^+ ions with the same laser damping as the two-ion case, the observed transitions shift to lower values with a wider hysteresis at $q_c, q'_c = 0.71, 0.60$.

The two-ion transition points q_c, q'_c are signatures of order-chaos transitions. The predicted value $q_c = 0.85$ of the forward branch follows from solutions of Eqs. (1) and (2) combined where $\alpha = 16.2$, $\Delta = -20$, $\chi = 64$, and $\gamma = 12.5$. Similarly, $q_c = 0.85$ results from Eq. (1) alone where $\Gamma = 2 \times 10^{-4}$, which is precisely the damping coefficient calculated⁷ from the above laser parameters. The transition was approached from $q = 0.3$ in steps of 0.01 under steady-state conditions where a random-number generator (range $\pm 0.4 \mu\text{m}$) shifts the final condition in a given step, providing the initial condition for the next. The almost perfect agreement in q_c leaves little doubt that the observed transition is from an ordered to a chaotic state. Figure 3 shows the hysteresis where the predicted (scattering rate $\propto \rho_{22}$) and observed count rate ratio for the two states are in good agreement, being ~ 5 . However, as yet, the predicted return branch does not exhibit condensation in this q interval because the high velocities arising in chaos require that our truncation errors be reduced.

In the experiments of Diedrich *et al.*,² phase transitions exhibiting hysteresis were observed in five laser-cooled Mg^+ ions, not only by varying q but also by varying Δ or χ as well. We suggest that these additional transitions are due also to order-chaos transitions where Δ and χ appear as control parameters. In work to be described elsewhere,⁷ we show that Eq. (2) can lead to *heating* instead of cooling at appropriate values of Δ and χ , even when the laser is tuned below the transition frequency—a result not anticipated in earlier single-ion laser cooling theories.⁶ Heating, of course, introduces a potential instability in Eq. (1), but numerical solutions suggest that chaos can result where ions are not expelled from the trap because the damping force, Eq. (2), saturates at high velocity. By varying Δ or χ , a hysteresis loop results when heating gives way to cooling and the ions return to the ordered state.

Finally, we mention that the numerical solutions of Eq. (1), the two-ion case, fall in the range of q_c values observed by Wuerker, Shelton, and Langmuir, namely,

$q_c = 0.645$ for 100 charged aluminum particles to $q_c = 0.866$ for 3 particles, the exact numbers being subject to the collisional damping Γ and the charge-to-mass ratio. In addition, hysteresis must have occurred even though it was not reported. Our calculations could be extended to more than two ions, providing additional tests, but the basic phenomenon of an order-chaos transition will remain. More interesting is the possibility of detecting the predicted frequency locking. Indeed, trapped ions might prove to be a testing ground for examining still other aspects of chaos not addressed here, particularly at the atomic level.

We are grateful to K. Jungmann for early contributions to the experiment, K. L. Foster for his technical expertise, W. Hensha for his perturbative analysis, and the U.S. Office of Naval Research for partial support.

¹R. F. Wuerker, H. Shelton, and R. V. Langmuir, *J. Appl. Phys.* **30**, 342 (1959).

²F. Diedrich, E. Peik, J. M. Chen, W. Quint, and H. Walther, *Phys. Rev. Lett.* **59**, 2931 (1987).

³D. J. Wineland, J. C. Bergquist, W. M. Itano, J. J. Bollinger, and C. H. Manney, *Phys. Rev. Lett.* **59**, 2935 (1987).

⁴P. Berge, Y. Pomeau, and C. Vidal, *Order Within Chaos* (Wiley, New York, 1984).

⁵J. Guckenheimer and P. Holmes, *Nonlinear Oscillations, Dynamical Systems, and Bifurcations of Vector Fields* (Springer-Verlag, New York, 1983).

⁶See, S. Stenholm, *Rev. Mod. Phys.* **58**, 699 (1986), for a review and references; D. J. Wineland and W. M. Itano, *Phys. Rev. A* **20**, 1521 (1979), and **25**, 35 (1982).

⁷R. G. DeVoe, J. Hoffnagle, and R. G. Brewer, to be published.

⁸With these terms, the radial equation reproduces the Duffing equation (Ref. 5). However, the radial equation by itself is not the route to chaos in the two-ion problem. Instead, it is the coupling of the r and z motions that is crucial.

⁹D. Ruelle and F. Takens, *Comm. Math. Phys.* **20**, 167 (1971).

¹⁰See B. A. Huberman and J. Crutchfield, *Phys. Rev. Lett.* **43**, 1743 (1979), for example.

¹¹See P. Cvitanovic, M. H. Jensen, L. P. Kadanoff, and J. Procaccia, *Phys. Rev. Lett.* **55**, 343 (1985), for example.

¹²W. Neuhauser, M. Hohenstatt, P. Toschek, and H. Dehmelt, *Phys. Rev. Lett.* **41**, 233 (1978), and *Phys. Rev. A* **22**, 1137 (1980).

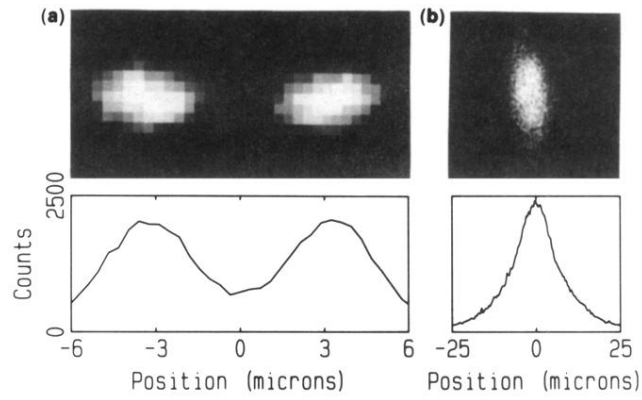


FIG. 5. Observed spatial patterns for two trapped Ba^+ ions in (a) the ordered state [$V_{\text{ac}}=401$ V(rms); $V_{\text{dc}}=59.6$ V] and (b) the chaotic state [$V_{\text{ac}}=680$ V(rms); $V_{\text{dc}}=0$].